56 Gb/s multi-band CAP for data center interconnects up to an 80 km SMF

Wei, Jinlong; Eiselt, Nicklas; Sanchez, Christian; Du, Ruoyang; Griesser, Helmut

Published in:
Optics Letters

Link to article, DOI:
10.1364/OL.41.004122

Publication date:
2016

Document Version
Peer reviewed version

56 Gb/s Multi-band CAP for Data Center Interconnects up to 80 km SMF

JINLONG WEI,[1,*] NICKLAS EISELT,[1,2] CHRISTIAN SANCHEZ,[3] RUOYANG DU,[4] HELMUT GRIESSER[5]

[1] *ADVA Optical Networking SE, Märzenquelle 1-3, 98617 Meiningen, Germany*
[2] *Technical University of Denmark, Department of Photonics Engineering, Ørsteds Plads, Build. 343, DK-2800, Denmark*
[3] *Aston Institute of Photonic Technologies (AIPT), Aston University, Birmingham, B4 7ET, UK*
[4] *Electrical Engineering Division, Department of Engineering, University of Cambridge, 9 J J Thomson Avenue, Cambridge, CB3 0FA, UK*
[5] *ADVA Optical Networking SE, Campus Martinsried, Fraunhoferstraße 9a, 82152 Martinsried/Munich, Germany*
**Corresponding author: JWei@advaoptical.com*

Received XX Month XXXX; revised XX Month, XXXX; accepted XX Month XXXX; posted XX Month XXXX (Doc. ID XXXXX); published XX Month XXXX

We present the first experimental demonstration of a 56 Gb/s multi-band CAP signal transmission over 80-km SMF link with zero overhead pre-FEC signal recovery and enhanced timing jitter tolerance for optical data center interconnects. © 2015 Optical Society of America

OCIS codes: *(060.0060) Fiber optics and optical communications, (060.4080) Modulation.*

http://dx.doi.org/10.1364/OL.99.099999

In the era of big data, the majority of the exponentially increasing Internet traffic passes through data centers, where thousands of servers are interconnected to store and process the data collaboratively. Higher order modulation formats in combination with coding and digital signal processing (DSP) are enabling technologies to handle the large amount of data traffic in data centers [1]. For intra-data center connections, intensity modulation and direct detection (IMDD) based short-reach fiber links (from 500-m, 2-km to 10-km standard single mode fiber (SMF)) are considered to support 400G with 8 channels of 50 Gb/s [2] or 4 channels of 100 Gb/s [3-6] each. Four level pulse amplitude modulation (PAM-4) and discrete multi-tone (DMT), namely IMDD based optical OFDM, are the dominant modulation formats considered for this application. The IEEE P802.3bs 400 GbE Task Force adopted PAM-4 as an industrial standard. Despite of this, another strong contender, multi-band carrierless amplitude and phase modulation (CAP) [3, 4, 7-9] has also shown excellent performance with respect to ease of implementation, enhanced chromatic dispersion tolerance (CD) and reduced DSP complexity compared to DMT.

Compared to intra-data center connects, inter-data center connects cover geographic areas up to 80 km and are well beyond the IEEE client optic standards. For such scenarios, coherent DP-M-QAM (M is 16 or 64) can offer efficient data transmission with a single wavelength capacity up to 200 Gb/s or even 400 Gb/s but might not satisfy the stringent requirements on cost, power and footprint. Alternatively, IMDD together with optically amplified dense wavelength division multiplexing (DWDM) systems in the 1550-nm transmission window are potential low-cost solutions by leveraging the ecosystem of short reach transceivers for a WDM link [10, 11]. Once again, PAM-4 and DMT are the dominant schemes considered [6, 10-12]. Demonstrations have been conducted to show that 400-Gb/s DMT on 8 channels [10] can successfully support 82 km of SMF transmissions and a single channel 112-Gb/s PAM-4 signal [12] transmission was demonstrated over 80-km SMF with the aid of dispersion compensating fiber and maximum likelihood sequence estimation. It is worth mentioning that other schemes such as fast OFDM (a variant of DMT) [13] and subcarrier modulation (SCM) or Nyquist QAM [14, 15] are feasible schemes for this scenario. Compared with SCM or QAM, CAP does not require an I/Q modulator in the transmitter, since CAP uses only orthogonal Hilbert pair shaping filters to up-convert baseband symbols without use of any RF carriers and mixers [3, 4]. Although single-band CAP signal transmission over 80-km SMF [8] and multi-band CAP WDM signal over 40-km SMF [9] have also been demonstrated, the single wavelength bit rate was only 40 Gb/s [8] and 45 Gb/s [9], respectively, and the OSNR performance have not been examined.

To the best of our knowledge, multi-band CAP has not been demonstrated with 56 Gb/s or 112 Gb/s per wavelength for inter-data center connects. In addition, as pointed out in [3], a CAP signal (especially sub-band signals at high frequencies) is sensitive to timing jitter or inaccurate clock recovery which results in non-ideal sampling and phase ambiguity (over 90 degrees phase rotations) might occur to the received signal constellation after matched filtering. Previous works either used training symbol based phase recovery [9] or has not clearly addressed this issue [4,7,8]. In this work, we propose the use of differential QAM encoding/decoding [16] together with a modified multi-modulus algorithm (MMA) based equalization to address the above-mentioned issues

efficiently. As the receiver is implemented in a complete blind manner, it achieves zero overhead and significantly relaxes requirements on timing recovery. Using this approach, double side-band (DSB) and vestigial side-band (VSB) 56-Gb/s Multi-band CAP signals transmission over a typical inter-data center transmission distances of 80-km SMF is evaluated in terms of OSNR performance and CD tolerance.

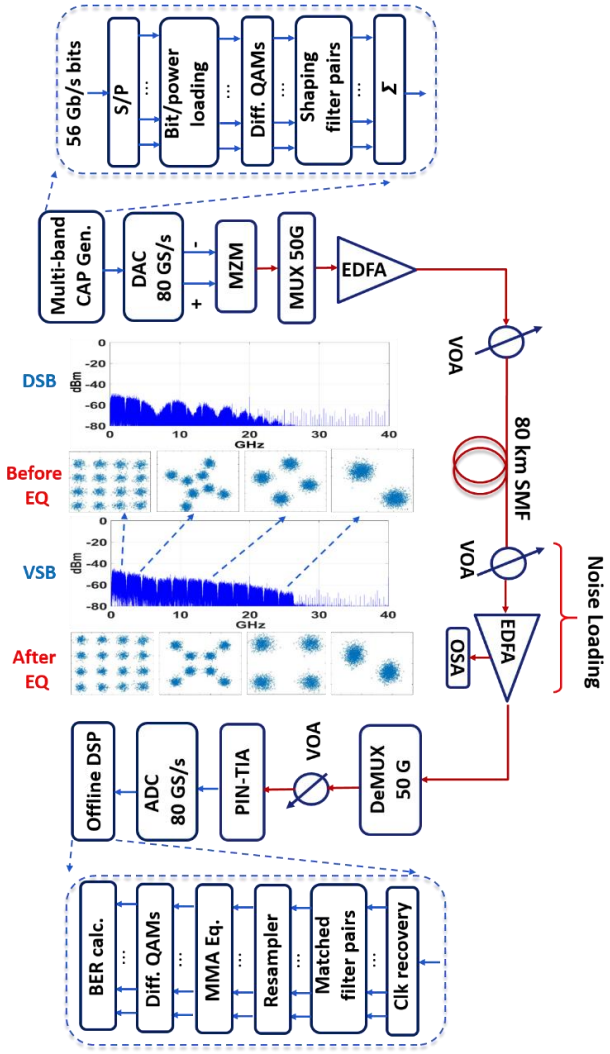

Fig. 1. Experimental setup for 56-Gb/s Multi-band CAP demonstrations for data center interconnects. The inset upper (lower) constellations are for representative sub-bands before (after) equalization with an OSNR of 37 dB.

The setup of a 56-Gb/s multi-band CAP link for inter-data center optical interconnects is illustrated by Fig. 1. The transmitter is composed of an offline multi-band CAP signal generator, an 80-GS/s digital to analog convertor (DAC), a tunable laser, and a differentially driven Mach-Zehnder intensity modulator (MZM). Following the MZM, a multiplexer (MUX) with a 50-G DWDM grid and a 3-dB bandwidth of approximately 39 GHz is adopted and its output is amplified by a booster erbium-doped fiber amplifier (EDFA). The tunable laser is tuned to generate a frequency offset between the laser frequency and the MUX center frequency, leading to a VSB multi-band CAP signal [9,10]. As shown in [10], the VSB signal can significantly increase the tolerance to fiber CD compared to the DSB case. The frequency offset is optimized in order to maximize the system performance. A variable optical attenuator (VOA) at the output of the EDFA adjusts the optical power launched into the fiber link. After transmission over 80-km SMF, a combined VOA and pre-amplifier EDFA is used to load optical noise onto the received signal. The resulting OSNR is measured by an optical spectrum analyzer (OSA) which is connected to the monitor port of the pre-amplifier. Then a 50-G de-multiplexer (De-MUX) further filters the optical signal and a VOA is used to optimize the input power injected into a 28-G PIN-TIA. The detected multi-band CAP signal is then converted into a digital signal by an ADC sampling at 80 GS/s. The digital signal is then sent to a computer and undergoes offline signal processing.

Fig. 1 also shows the detailed procedure of the DSP of the transmitter multi-band CAP signal generator and the offline receiver. The transmitter offline DSP first performs a serial to parallel (S/P) conversion to the input bit stream. At start-up, the system estimates the SNR of each sub-band signal by transmitting a 2-GBaud DQPSK signal at each sub-band simultaneously, and then, based on these values, performs a Levin-Campello bit/power loading algorithm with fixed bit rate. Each sub-band adopts an assigned differential encoding scheme varying from DBPSK, DQPSK to differential 32-QAM to convert bit streams into complex symbols. This is illustrated in an inset of Fig.1, where constellation diagrams for the 1st, 2nd, 7th and 12th sub-band received signal after ADC are presented, respectively. The upper (lower) constellations are obtained before (after) equalization. The symbol rate for each sub-band is set to 2 GBaud, which is also the bit rate granularity for bit loading. In total 12 sub-bands are transmitted, which cover a total bandwidth of 26.4 GHz, as indicated in the spectrum inset of Fig. 1. The mapped symbols of each sub-band are then pulse shaped by using an orthogonal square-root raised cosine shaping filter pair (inphase and quadrature) with roll-off coefficient of 0.1 at its assigned center frequency [3]. The resulting symbols of all sub-bands are then added, clipped to achieve a peak to average power ratio of 11 dB, and quantized to the amplitude range required by the DAC.

The receiver offline DSP is roughly an inverse of the transmitter DSP process. The receiver DSP starts with a clock recovery which tries to obtain the optimum sampling point for each sub-band signal. Following filter pairs matched to the transmitter shaping filter pairs are used to separate the sub-band signals. Afterwards, the signal is resampled to two samples per symbol, which facilitates the implementation of a simple blind 14-tap T/2 spaced (T is the symbol time period) MMA algorithm based feed-forward equalizer (FFE) [17]. The equalized complex sub-band symbols are then converted into bits by the following differential QAM decoders. Finally, the bit error rate (BER) is the result of a one-on-one comparison between the transmitted and the recovered bits. The use of differential QAM encoding and decoding can effectively address the 90 degree phase ambiguity issue caused by phase rotation from a timing error [3]. As a result, no training symbols or sequences are needed for equalization and signal recovery can be achieved without additional overhead.

First a system optimization is performed for the proposed link and then measured OSNR for the 56-Gb/s Multi-band CAP link are presented. The system performance is mainly determined by the optical link including the MZM intensity modulator, the relative frequency offset between the VSB multi-band CAP signal carrier and the (De-)MUX center frequency, and the optical launch power.

Fig. 2 shows the MZM power transfer function and the dependency of the SNR on the MZM driving voltage. As shown in Fig. 2(a), the MZM has a switching voltage of approximately Vπ = 5 V. In contrast, the DAC output has a swing of only 550 mV as indicated by the rectangular block in Fig. 2(a), which is about one ninth of the switching voltage leading to a low dynamic range modulation. In order to maximize the SNR, the operation point has to be pushed to the regime close to the power null point to avoid a strong DC in the optical multi-band CAP signal. This is verified by Fig. 2(b), which clearly shows the improved electrical SNR (and equivalently the improvement in the extinction ratio) of each sub-band by moving the bias close to the power null point until an optimum bias voltage is achieved. Above the optimum bias voltage the achievable electrical SNR dominates system performance while below the optimum bias the MZM nonlinearity as shown in Fig. 2(a) overwhelms and significantly degrades performance. Thus the electrical SNR saturates as signal DC is further suppressed. The identified optimum bias is approximately -2.6 V. Therefore, all the following measurements are based on the identified optimum MZM bias voltage. Note that the MZM output power is quite low, which can be compensated by a booster EDFA. The near null point bias of MZM leads to an OSNR of approximately 40 dB for the booster EDFA output. The EDFA can be shared among all wavelengths in the system and thus it avoids the use of a high bandwidth linear driver amplifier for every channel, which is normally costly and power consuming.

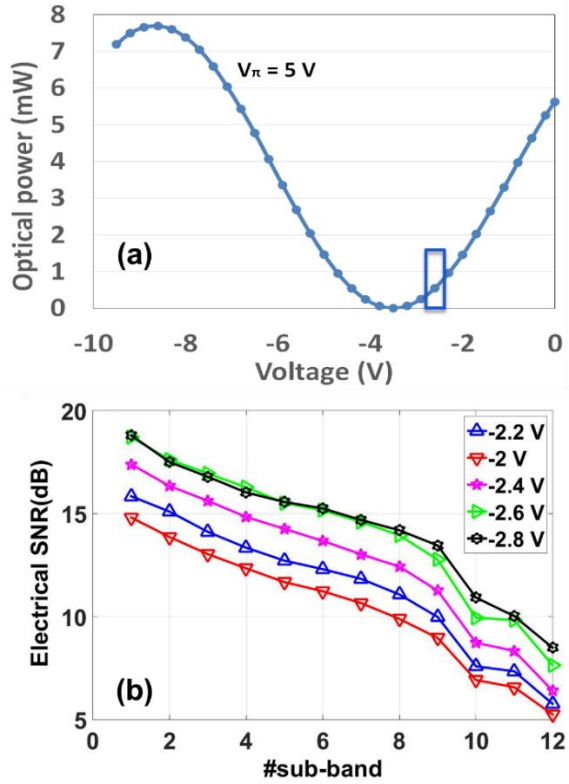

Fig. 2. (a) Measured MZM transfer function, and (b) measured electrical SNR of each sub-band subject to different bias voltages for the optical back-to back case. The OSNR is fixed at 31.5 dB.

In order to increase the system tolerance to chromatic dispersion, VSB is applied and implemented by changing the laser frequency to introduce an offset relative to the center frequency of the MUX and De-MUX. Fig. 3 presents the dependency of the system's overall BER on the frequency offset for 80-km transmission. The BER decreases with increasing the frequency offset until an optimum value is achieved. Beyond this point, the BER rises quickly. Ideally the optimum performance can be obtained if an optical single-side band (SSB) is achieved, which can avoid frequency notches resulting from CD and the beating between upper and lower side bands of a DSB signal upon square-law detection, as indicated by inset of Fig. 1. Here we try to approach this by simple filtering, leading to a VSB signal. Fig. 1 insets clearly show that VSB can mitigate frequency notches effectively although slight residential frequency notches exist. There exists an optimum region of approximately 6 GHz (from 14 GHz to 20 GHz) where low BERs can be achieved. 20 GHz frequency offset gives rise to the best BER thus this value is adopted for the following measurements. However, a further increased frequency offset introduces distortion to the side-band need to be preserved and causes a worse performance.

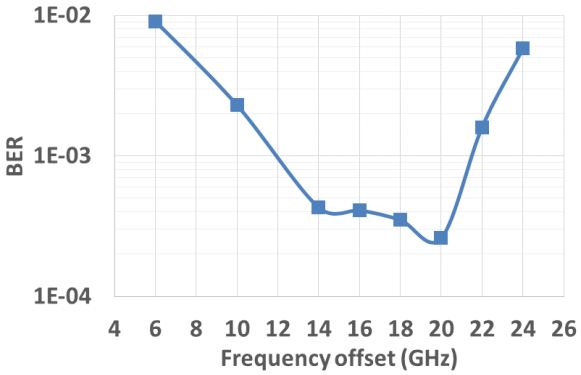

Fig. 3. BER versus frequency offset for the 80 km SMF case. The OSNR is fixed at 35.6 dB.

Fig. 4 examines the relationship between the system performance and the optical launch power. It clearly shows that there exists a launch power region from 2 dBm to 8 dBm where lower BERs can be obtained, with 4 dBm as an optimum launch power. For lower launch powers, the system is limited by the achievable OSNR of the received signal, as indicated by Fig. 4. For high launch powers, the system suffers from fiber nonlinearities. Note that the input power to the PIN-TIA is always carefully adjusted by the VOA prior to it to avoid limiting. The OSNR begins to decrease with increasing launch power at the power regime beyond 8 dBm.

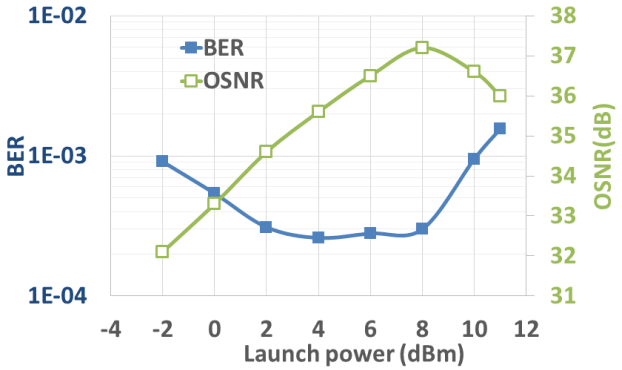

Fig. 4. BER versus launch power for VSB multi-band CAP over 80 km SMF. The corresponding OSNR is also measured.

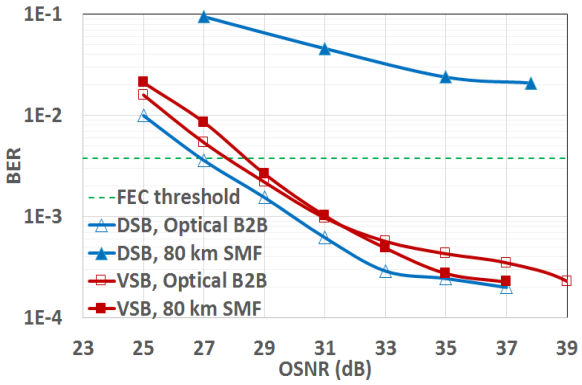

Fig. 5. BER versus OSNR for both DSB and VSB multi-band CAP over optical bac-to-back and 80-km SMF links.

Having optimized the key parameters of the optical link, Fig. 5 presents the performance of both the DSB and the VSB 56 Gb/s multi-band CAP systems for the optical back-to-back (B2B) and an 80 km SMF link. For the optical B2B case, DSB multi-band CAP achieves the highest OSNR sensitivity of approximately 27 dB at a BER FEC threshold of 3.8×10^{-3}. The VSB link shows about 0.7 dB penalty compared to DSB, mainly because the VSB filtering causes a drop in the achievable SNR at some middle sub-bands [10]. For both DSB and VSB, the BER decreases with increasing OSNR until an error floor appears, which may be attributed to the transceiver nonlinearity and the quantization noise from DAC and ADC. For the 80-km SMF case, VSB multi-band CAP shows a small OSNR penalty of only 0.5 dB compared to its optical B2B counterpart, while DSB fails to support transmission over 80 km SMF for the assumed FEC threshold. This is mainly because the DSB multi-band CAP scheme suffers from strong CD induced frequency notches as already explained before, while VSB can almost avoid such degradation. Fig. 6 shows the bit loading maps for both DSB and VSB cases over 80 km SMF, which clearly indicates that very high order modulation up to differential 32-QAM has to be used in the low frequency band while high frequencies cannot be used for DSB, due to CD-induced frequency notches as shown in the spectrum inset of Fig. 1. VSB allows more moderate modulation orders for most sub-bands. This also explains the small penalty of the VSB multi-band CAP signal transmission over 80 km SMF.

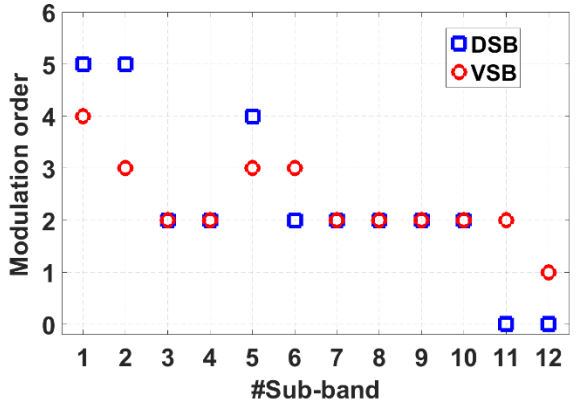

Fig. 6. Bit loading maps for both DSB and VSB multi-band CAP signals over 80 km SMF. The VSB is based on a frequency offset of 20 GHz. The baudrates for both cases are 2 GBaud.

We have experimentally demonstrated a 56-Gb/s multi-band CAP system for data center interconnects. The results show that VSB-based multi-band CAP signal can be successfully transmitted over 80 km SMF with a penalty of 0.5 dB and requires approximately 28 dB OSNR at a BER of 3.8×10^{-3}.

Funding. European Union Seventh Framework Programme (623515; 608363); EU H2020 (659950)

Acknowledgment. We thank Dr. Annika Dochhan and Aymen Fakhfakh from ADVA Optical Networking SE, Germany, for useful discussions and suggestions.

References

1. J. L. Wei, Q. Cheng, R. V. Penty, and I. H. White, IEEE Commun. Magazine, **53**, 182 (2015).
2. N. Eiselt, H. Griesser, J. L. Wei, A. Dochhan, R. Hohenleitner, M. Eiselt C. Neumeyr, J. J. V. Olmos, and I. T. Monroy, accepted by ECOC 2016.
3. J. L. Wei, Q. Cheng, D. G. Cunningham, R. V. Penty, and I. H. White,, J. Lightwave Technol. **33**, 415 (2015).
4. M. I. Olmedo, T. Zuo, J. B. Jensen, Q. Zhong, X. Xu, S. Popov, and I. T. Monroy, J. Lightwave Technol., **32**, 798 (2014).
5. P. Dong, J. Lee, Y.-K. Chen, L. L. Buhl, S. Chandrasekhar, J. H. Sinsky, K. Kim, in *Proc. OFC 2015* (Optical Society of America, 2012), Paper Th5B.4.
6. W. Yan, T. Tanaka, B. Liu, M. Nishihara, L. Li, T. Takahara, Z. Tao, J. C. Rasmussen. T. Drenski, in *Proc. OFC 2013* (Optical Society of America, 2013), Paper OM3H.1.
7. R. Puerta, M. Agustin, Ł. Chorchos, J. Toński, J.-R. Kropp, N. Ledentsov Jr., V.A. Shchukin, N.N. Ledentsov, R. Henker, I. T. Monroy, J.J. Vegas Olmos and J.P. Turkiewicz, in *Proc. OFC 2016* (Optical Society of America, 2016), Paper PDP Th5B.5,.
8. Y. Gao, Q. Zhuge, W. Wang, X. Xu, J. M. Buset, M. Qiu, M. M.-Osman, M. Chagnon, F. Li, L. Wang, C. Lu, A.P. T. Lau, and D. V. Plant, Opt. Express, **23**, 11412 (2015).
9. J. Zhang, J. Yu, F. Li, N. Chi, Z. Dong, and X. Li, Opt. Express, **21**, 18842 (2013).
10. A. Dochhan, H. Griesser, N. Eiselt, M. H. Eiselt, und J. P. Elbers, J. Lightw. Technol., **34**, S.491 (2016).
11. N. Eiselt, J. L. Wei, H. Griesser, A. Dochhan1, M. Eiselt, J.-P. Elbers, J. J. Vegas Olmos, and I. T. Monroy, in *Proc. OFC 2016* (Optical Society of America, 2016), Paper W1K.5.
12. D. Sadot, G. Dorman, A. Gorshtein, E. Sonkin, and O. Vidal, in *Proc. OFC 2015* (Optical Society of America, 2015), Paper Th2A.67.
13. E. Giacoumidis, A. Tsokanos, C. Mouchos, G. Zardas, C. Alves, J. L. Wei, J. M. Tang, C. Gosset, Y. Jaouën, I. Tomkos, IEEE J. Opt. Commun. Netw, **4**, 724 (2012).
14. M. Sezer Erkılınç, Manoj P. Thakur, Stephan Pachnicke, Helmut Griesser, John Mitchell, Benn C. Thomsen, Polina Bayvel, and Robert I. Killey, J. Lightwave Technol., **34**, 1158, (2016).
15. K. Zou, Y.Zhu, F. Zhang, and Z. Chen, Opt. Lett., **41**, 2767 (2016).
16. W. J. Weber, IEEE Trans. Communications, **26**, 385 (1978).
17. L. M. Garth, J. Yang, and J.-J. Werner, IEEE Trans. Communications, **49**, 455 (2001).

Full Citation List

1 J. L. Wei, Q. Cheng, R. V. Penty, and I. H. White, “400 Gigabit Ethernet using advanced modulation formats: performance, complexity, and power dissipation,” IEEE Commun. Magazine, vol. 53, no. 2, pp. 182-189, 2015.

2 N. Eiselt, H. Griesser, J. L. Wei, A. Dochhan, R. Hohenleitner, M. Eiselt C. Neumeyr, J. J. V. Olmos, and I. T. Monroy, “'Experimental Demonstration of 56 Gbit/s PAM-4 over 15 km and 84 Gbit/s PAM-4 over 1 km SSMF at 1525 nm using a 25G VCSEL,” accepted by ECOC 2016.

3 J. L. Wei, Q. Cheng, D. G. Cunningham, R. V. Penty, and I. H. White,, “100 Gb/s Hybrid Multiband (HMB) CAP/QAM signal transmission over a single wavelength,” J. Lightwave Technol. vol.33, no. 2, pp. 415-423, 2015.

4 M. I. Olmedo, T. Zuo, J. B. Jensen, Q. Zhong, X. Xu, S. Popov, and I. T. Monroy, “Multiband carrierless amplitude phase modulation for highcapacity optical data links,” J. Lightwave Technol., vol. 32, no. 4, pp. 798–804, 2014

5 P. Dong, J. Lee, Y.-K. Chen, L. L. Buhl, S. Chandrasekhar, J. H. Sinsky, K. Kim, “Four-channel 100-Gb/s per channel Discrete Multi-Tone modulation using silicon photonic integrated circuits, ” Proc. OFC 2015, Paper Th5B.4.

6 W. Yan, T. Tanaka, B. Liu, M. Nishihara, L. Li, T. Takahara, Z. Tao, J. C. Rasmussen. T. Drenski “100 Gb/s optical IM-DD transmission with 10G-class devices enabled by 65 GSamples/s CMOS DAC core,” Proc. OFC 2013, Paper OM3H.1, Mar. 2013.

7 R. Puerta, M. Agustin, Ł. Chorchos, J. Tońsk, J.-R. Kropp, N. Ledentsov Jr., V.A. Shchukin, N.N. Ledentsov, R. Henker, I. T. Monroy, J.J. Vegas Olmos and J.P. Turkiewicz, “107.5 Gb/s 850 nm multi- and single-mode VCSEL transmission over 10 and 100 m of multi-mode fiber,” Proc. OFC 2016, Paper PDP Th5B.5

8 Y. Gao, Q. Zhuge, W. Wang, X. Xu, J. M. Buset, M. Qiu, M. M.-Osman, M. Chagnon, F. Li, L. Wang, C. Lu, A.P. T. Lau, and D. V. Plant, “40 Gb/s CAP32 short reach transmission over 80 km single mode fiber,” Opt. Express, vol. 23, no. 9, pp. 11412-11423, Apr. 2015.

9 J. Zhang, J. Yu, F. Li, N. Chi, Z. Dong, and X. Li, “11 × 5 × 9.3 Gb/s WDM-CAP-PON based on optical single-side band multi-level multi-band carrier-less amplitude and phase modulation with direct detection,” Opt. Express, vol. 21, no. 16, pp. 18842–18848, 2013.

10 A. Dochhan, H. Griesser, N. Eiselt, M. H. Eiselt, und J. P. Elbers, „Solutions for 80 km DWDM Systems“, Journal of Lightwave Technology, vol. 34, no. 2, S. 491–499, Jan. 2016.

11 N. Eiselt, J. L. Wei, H. Griesser, A. Dochhan1, M. Eiselt, J.-P. Elbers1, J. J. Vegas Olmos, and I. T. Monroy, “First Real-Time 400G PAM-4 Demonstration for Inter-Data Center Transmission over 100 km of SSMF at 1550 nm,” OFC 2016, Paper W1K.5, Mar. 2016.

12 D. Sadot, G. Dorman, A. Gorshtein, E. Sonkin, and O. Vidal, “Single channel 112 Gb/s PAM4 at 56Gbaud with digital signal processing for data center applications,” Proc. OFC 2015, Paper Th2A.67.

13 E. Giacoumidis, A. Tsokanos, C. Mouchos, G. Zardas, C. Alves, J. L. Wei, J. M. Tang, C. Gosset, Y. Jaouën, I. Tomkos, “Extensive Comparisons of Optical Fast-OFDM and Conventional Optical OFDM for Local and Access Networks,” Journal of Optical Communications and Networking, vol. 4, no. 10, pp. 724-733, Oct. 2012.

14 M. Sezer Erkılınç, Manoj P. Thakur, Stephan Pachnicke, Helmut Griesser, John Mitchell, Benn C. Thomsen, Polina Bayvel, and Robert I. Killey, "Spectrally Efficient WDM Nyquist Pulse-Shaped Subcarrier Modulation Using a Dual-Drive Mach–Zehnder Modulator and Direct Detection," J. Lightwave Technol. no. 34, pp. 1158-1165, Feb. 2016.

15 K. Zou, Y.Zhu, F. Zhang, and Z. Chen, "Spectrally efficient terabit optical transmission with Nyquist 64-QAM half-cycle subcarrier modulation and direct detection," Opt. Lett., vol. 41, no. 12, pp. 2767-2770, Jun. 2016.

16 W. J. Weber, “Differential encoding for multiple amplitude and phase shift keying systems” IEEE Transactions on Communications, vol. 26, no. 3, pp. 385 – 391, 1978.

17 L. M. Garth, J. Yang, and J.-J. Werner, “Blind equalization algorithms for dual-mode CAP-QAM reception,” IEEE Trans. Communications, vol. 49, no. 3, pp. 455-466, Mar. 2001.